THE ASTROPHYSICAL JOURNAL, 490:L161–L164, 1997 December 1
© 1997. The American Astronomical Society. All rights reserved. Printed in U.S.A.

AN UNUSUAL X-RAY BURST FROM THE GLOBULAR CLUSTER M28

E. V. GOTTHELF[1]
Laboratory for High Energy Astrophysics, NASA/GSFC, Greenbelt, MD 20771
AND
S. R. KULKARNI
Division of Physics, Mathematics, and Astronomy, 105-24, California Institute of Technology, Pasadena, CA 91125
Received 1997 August 4; accepted 1997 September 16; published 1997 November 4

ABSTRACT

We report the discovery of an unusual X-ray burst from the direction of the globular cluster M28 using data acquired with *ASCA*. The burst was recorded by all four *ASCA* telescopes and displays a fast ($\lesssim$70 ms) rise followed by an exponential decay (τ = 7.5 s) and a steady afterglow that lasts between 800 and 3250 s. The image of the burst is consistent with an *ASCA* point source and is centered on quiescent X-ray emission from the core of M28. The burst temporal profile is similar to type I bursts emitted by accreting neutron stars of low-mass X-ray binaries (LMXBs). We argue that the burst arises from a LMXB that is located in the core of M28. The burst is unique in two ways: it is intrinsically subluminous, $\sim 0.02 L_{\rm E}$, and more importantly it originates from a source whose quiescent luminosity is fainter than that of the known cluster bursters by 3 orders of magnitude. We suggest that this burst is from a highly magnetized neutron star accreting at a low rate. These accreting systems may account for the mysterious low-luminosity X-ray sources in globular clusters.

Subject headings: stars: individual (M28, PSR B1821−24) — stars: neutron — X-rays: bursts — X-rays: stars

1. INTRODUCTION

The low-mass X-ray binaries (LMXBs) are the brightest X-ray sources in the sky. About 124 are known, ~40 of which show type I bursts (Lewin, van Paradijs, & Taam 1993). These bursts are characterized by a sharp rise time and a spectrum that becomes softer as the burst evolves. The bursts have been interpreted as cooling of a thin layer of material on the surface of neutron stars that is heated by unstable nuclear fusion within this layer (Woosley & Taam 1976; Maraschi & Cavaliere 1977). The peak luminosity appears to have a small dispersion—less than a factor of 10 with a maximum value equal to the Eddington luminosity, $L_{\rm E} \sim 10^{38}$ ergs s^{-1}. A disproportionate number of LMXBs are found in the Galactic globular clusters, and all these have exhibited a type I burst (Dotani et al. 1990).

A day long observation of the globular cluster M28 was conducted with *ASCA* (Tanaka et al. 1994) on 1995 March 29 UT. The original motivation was to search for X-ray pulsations from the known 3 ms radio pulsar PSR B1821−24 (Lyne et al. 1987). These pulsations were subsequently detected (Saito et al. 1997). Recently, during the course of verification of a timing package, we analyzed this data. In the process we discovered an unusual X-ray flash, the analysis of which is reported in this Letter.

2. OBSERVATIONS

The *ASCA* satellite consists of four coaligned telescopes, each of which is a conical foil mirror coupled to one of two types of focal plane sensors, the two Solid State Imaging Spectrometers (SIS-0 and SIS-1) or the two Gas Imaging Spectrometers (GIS-2 and GIS-3). The SIS detectors are sensitive to photons in the 0.4–10.0 keV energy band with a nominal spectral resolution of 2% at 6 keV, scaling as $\sim E^{-1/2}$. The angular resolution of the SIS is ~1′, limited by the mirror optics. The SIS data were acquired in the "4-CCD" mode, using 16 s integrations, with the 22′ × 22′ SIS field of view centered on the core of the M28 cluster.

The GIS detectors have a relatively modest spectral resolution of 8% at 6 keV, in comparison to the SIS, with a larger effective area at higher energies. The temporal resolution is also higher, 61 μs or 0.5 ms, depending on the mode selected. The images formed by the GIS suffers from an energy-dependent blur, which results in an effective angular resolution of 3′. The GIS data were edited using the standard "REV1" processing criteria to exclude periods of high background contamination. The SIS data were time filtered using the GIS good time intervals to directly compare the light curves from both instruments. The final effective exposure time is ~37 ks per detector.

3. RESULTS

The *ASCA* image of the M28 region obtained using the entire data set contains a single unresolved source, AX J18245−2451. This source is located at the light centroid of the globular cluster M28 and has been studied in detail by Saito et al. (1997). We constructed light curves using photons from a 12′ diameter aperture centered on AX J18245−2451 and found a flash, lasting tens of seconds, followed by an afterglow. The profile of the burst is essentially identical in all instruments (Fig. 1). The background light curves from each detector show no appreciable rise in the overall count rate during the flash or the afterglow. The summed background light curve is shown in Figure 1 and contains photons from a concentric annulus of radius 12′–20′ (GIS) and more than 12′ (SIS).

The background particle flux rate during the burst interval, as measured by the GIS radiation belt monitor, shows no unusual activity during this period. A careful study of the GIS scaler (discriminator) rates, which record the number of detections in each GIS before any detailed processing is done, also show no abnormal behavior. The scaler rates during the burst are at no time high enough to warrant dead-time correction. As expected, the burst count rates measured by each de-

[1] Universities Space Research Association.

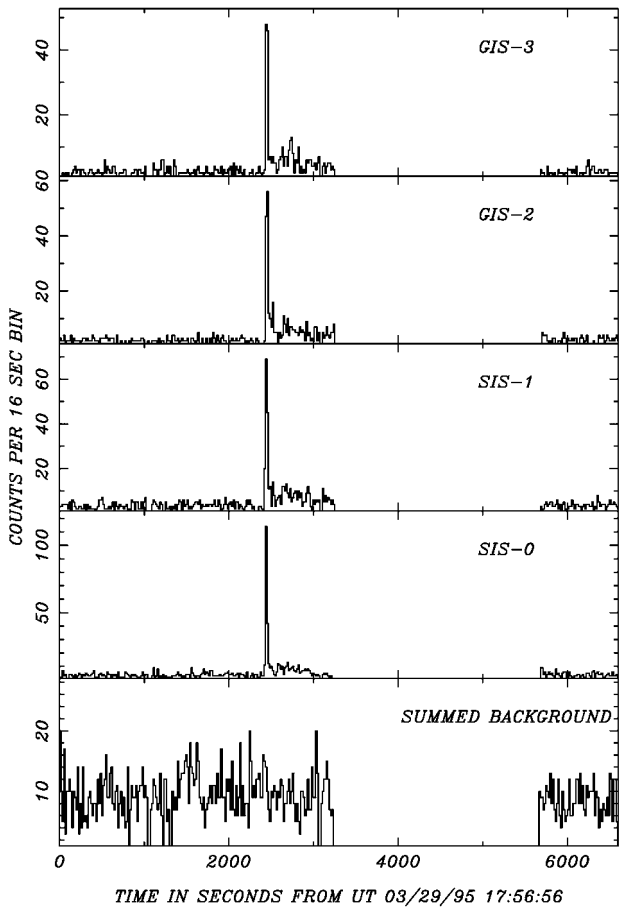

FIG. 1.—All four telescopes aboard *ASCA* observed the burst from M28. The burst profile is essentially identical in all instruments with a bright peak and a distinct afterglow signature. These light curves are binned in 16 s steps. The amplitude of the burst (as defined by the height of the peak bin) is determined by the large, undersampled, binning and is somewhat arbitrary. No appreciable rise in the background rate accompanied the burst; the burst is coincident with the quiescent flux from the core of M28. The data gap between the interval of 3.2 to 5.6 ks is due to SAA passage.

tector are not the same. This is because the four mirrors are not quite coaligned, and a source will fall at different off-axis angles for each mirror and thus suffer a varying amount of mirror vignetting (geometric shadowing). A second reason is that the relative detector efficiency is a strong function of position. The combined effect of the two is typically ~30%. Indeed, we find that the relative burst fluence measured from each detector is consistent with that expected for a cosmic (i.e., a distant) source imaged through the telescopes; the relative count rates for the burst are identical to those measured for the quiescent emission, within counting statistics and spectral differences.

Figure 2 (Plate L10) shows the combined SIS (SIS-0 + SIS-1) images and spectra of AX J18245−2451 obtained during the time intervals defined in Table 1: preburst, flash, afterglow, and postburst. The images are centered on AX J18245−2451 and display the 22′ × 22′ field of view of the SIS. The burst and afterglow photons form an image that, within the photon counting errors, is a point source with the same pixel centroid as AX J18245−2451; the 95% confidence radius of the burst localization is 40″ (see Gotthelf 1996 for details on measurement accuracy with the SIS).

The facts presented so far—(1) the detection of the burst in all four detectors, (2) the absence of any abnormal behavior in the background rate, and (3) the consistency of the image of the burst in each detector, including the variation in fluence expected from telescope vignetting—lead us to conclude that the burst is cosmic in origin. This conclusion motivated us to carry out a detailed analysis of the burst.

For each of the four sub-time intervals specified in Table 1 we created a spectrum from photons extracted from a 12′ diameter circular region centered on the image peak. These spectra are displayed in Figure 2. To compare spectra from different time intervals we have normalized them by duration and plotted them autoscaled to the peak value. The burst rate is almost 2 orders of magnitude higher than the quiescent rate. Even without any sophisticated analysis we note that the spectrum of the burst is distinctly different from that of the quiescent emission. The results discussed here are identically reproduced by the GIS data.

As with the SIS data, GIS photons within a 12′ diameter circular region centered on AX J18245−2451 were extracted. The burst profile derived from the combined GIS data is shown in Figure 3 (Plate L10). The rise of the burst is unresolved. A photon-by-photon arrival time analysis of the high time resolution GIS data yields a turn-on time of < 70 ms. The burst decay signal is well represented by an exponential model, $I(t) = I_p e^{-t/\tau} + I_a S(t) + I_q$, where $S(t)$ is the step function, $S(t) = 0, t < 0$, $S(t) = 1, t > 0$, and the subscripts p, a, and q refer to the peak, afterglow, and quiescent (preburst) counting rates. Fitting the data to this functional form we obtain $I_p = 28.0$ counts s^{-1}, $I_a = 0.20$ counts s^{-1}, $I_q = 0.08$ counts s^{-1}, and $\tau = 7.5$ s; this model is displayed in Figure 3 (*solid line*). The start time of the first significant burst emission measured by the two instruments is consistent with counting statistics (roughly the inverse of the count rate). The estimated uncer-

TABLE 1
M28 OBSERVATION LOG AND BURST TIME INTERVALS

Interval	Start Time (UT)	Exposure[a] net (total) (s)	Counts[b]	Rates (counts s^{-1})
Observation	28/03/95 17:23:36	74220(207328)	6654	0.09
Preburst	28/03/95 17:23:36	62581(181664)	5137	0.08
Burst	29/03/95 18:37:33	90(90)	212	2.21[c]
Afterglow	29/03/95 18:38:18	1440(1528)	400	0.28
Postburst	29/03/95 18:51:02	10109(24036)	905	0.09

[a] Screened (i.e., good time interval, or GTI) and total exposure time from both GIS sensors.

[b] Total photons falling within a 6′ radius aperture centered on the X-ray source (both GIS sensors).

[c] Peak rate is 28 counts s^{-1}.

tainty in the onset of the burst is about 40 ms. The afterglow increases the quiescent (preburst) count rate ~2.5 times and lasts between 800 and 3250 s; the gap in the data is due to Earth block.

Comparison of the burst profile in the hard band (>2.0 keV) and soft band (<2.0 keV; see Fig. 3) shows some indication of spectral evolution from the initial soft impulse. Specifically, the spectrum is seen to soften (i.e., more photons at lower energies relative to higher energies) as the burst evolves.

Spectral fits to the mean burst spectrum obtained from the two GISs are presented in Table 2. The background is a negligible contribution during this interval. We fitted several standard models to the data, all of which produced reasonable fits. This is not surprising given the small number of counts. It is noteworthy that all three models require a best-fit $N_{\rm H}$-value larger than that obtained by Saito et al. (1997) from analysis of the 3 ms pulsar data. Saito et al.'s $N_{\rm H}$-value of 2.8×10^{21} cm^{-2} is consistent with other measures of the interstellar absorption expected to the cluster M28. Thus, we conclude that there is an additional absorption internal to the bursting source.

TABLE 2

M28 Burst GIS Spectral Fits[a]

Model	Continuum (Γ or kT)	$N_{\rm H}^{\rm I}$[b] ($\times 10^{22}$ cm^2)	Fluence[c] (ergs cm^{-2})	χ^2_ν (ν)
Power Law	$3.7^{+1.2}_{-0.9}$	$2.2^{+1.2}_{-1.0}$	1.1×10^{-8}	0.9 (12)
Blackbody	$0.6^{+0.1}_{-0.1}$	$0.35^{+0.9}_{-0.3}$	7.7×10^{-9}	1.3 (12)
$R - S$	$1.6^{+1.0}_{-0.5}$	$1.3^{+2.6}_{-0.9}$	1.1×10^{-8}	1.1 (12)

[a] GIS-2 and GIS-3 photons collected using a 6 arcmin aperture centered on the source with no background subtraction (assumed negligible). Spectral fits are in the 1.0–10.0 keV range. Errors are 90% confidence region for a single interesting parameter.

[b] Intrinsic absorption, after allowing for an interstellar absorption of 2.9×10^{21} cm^2 (from Saito et al. 1997).

[c] The unabsorbed fluence at the front of the telescope, integrated during the 45 s burst interval.

4. DISCUSSION

The duration of the flash is so short that we can safely exclude stellar flares (Greiner, Duerbeck, & Gershberg 1994, pp. 1-456) from an active star such as UV Ceti or a T Tauri (young) star. Our flash was not coincident in time with any known gamma-ray burst, making it unlikely to be an X-ray precursor. This flash bears some similarity to the flashes reported from analysis of the database of the X-ray satellite *Einstein* (Gotthelf, Hamilton, & Helfand 1996). But the sky distribution of the *Einstein* flashes does not suggest a globular cluster origin. We note that both the temporal and spectral properties of our flash are similar to those of type I bursts. Furthermore, the flash is coincident with the core of a globular cluster and clusters are known to be relatively abundant in LMXBs. To our knowledge all LMXBs in clusters have exhibited a type I burst (Dotani et al. 1990). Thus, we adopt the simplest hypothesis, viz., that this is a type I burst originating in the globular cluster M28.

Using the mean spectrum for the flash (Table 2) we obtain a peak flux of 1.4×10^{-9} ergs cm^{-2} s^{-1}, which translates to an (assumed) isotropic luminosity of $L_B \sim 4.3 \times 10^{36}$ ergs s^{-1}; the distance to M28 is assumed to be 5.1 kpc (Rees & Cudworth 1991). The total energy in the burst is $E_B \sim 3.1 \times 10^{37}$ ergs. Almost all type I bursts reported in the literature have peak luminosities $fL_{\rm E}$ with f ranging from more than 0.1 to 1, where $L_{\rm E} \sim 2 \times 10^{38}$ ergs s^{-1} is the Eddington luminosity for a neutron star. Our burst appears to have $f \sim 0.02$. This may appear to be in conflict with our conclusion that the burst under discussion is a type I burst. However, below, we argue that this is not a fatal objection.

type I bursts are understood to be thermonuclear instabilities of the accreted matter on neutron stars. Once a critical column density $C_{\rm cr}$ is reached, nuclear fusion produces far more heat than can be radiated away. This results in the layer getting heated till expansion sets in. The resulting cooling accounts for the softening of the spectrum as the burst progresses. At any given point on the surface of the neutron star, the critical column density is a function of the composition (including metallicity) of the accreted gas, the core temperature of the neutron star, and the *local* accretion rate (Taam & Picklum 1978; Joss & Li 1980; Fujimoto, Hanawa, & Miyaji 1981). $C_{\rm cr}$ (Fujimoto et al. 1981; Bildsten & Brown 1997) varies from 2×10^8 to 2×10^7 g cm^{-2} as the core temperature varies from $10^{7.5}$ to 10^9K.

Strong magnetic fields force the accretion to polar cap regions, thereby changing the local accretion rate. This fact explains why accreting X-ray pulsars (which are highly magnetized neutron stars) are not seen to burst and likewise why bursters do not pulse. For a given source, $C_{\rm cr}$ is not expected to be highly time dependent. For values of $C_{\rm cr}$ applicable to most bursters, the observed range in f translates to an inference that the bursts are from a substantial portion, 10% to 100%, of the surface of the neutron star. This inference fits in well with our ideas that LMXBs are magnetically weak neutron stars and thus there is little impediment to prevent the spread of accreted material.

There is an alternative explanation for subluminous type I bursts. Garcia & Grindlay (1987) noted that a type I burst from 4U 2129+47 had an even lower f-value, ~0.002. They persuasively argue that 4U 2129+47 is a LMXB whose thick accretion disk obscures the neutron star from our sight. From our vantage point we only see a fraction of the quiescent and the burst emission that is scattered by the electrons in the corona. This accounts for the small value of f. This model also explains two other peculiarities of the 4U 2129+47 burst: a longer rise time (6 s instead of the usual less than 1 s) and the higher effective temperature, ~3 keV instead of $\lesssim$2 keV. Scattering allows multipath propagation, which then accounts for the longer rise time. Inverse Compton scattering of photons by the hot electrons in the corona also boosts the energy of the incident photon.

However, the flash reported here has a soft spectrum and a short rise time and appears to be no different from a typical type I burst. Thus, we conclude that our flash is a type I burst but intrinsically subluminous. If so, we are forced to the conclusion that material from only a small area of the neutron star, between 0.1% and 1%, was involved in this burst, depending on the value of $C_{\rm cr}$ we adopt. For a low-luminosity source, $C_{\rm cr}$ is higher, and thus we prefer the smaller value for the area. The accreted material is probably confined by a strong magnetic field. With such a small area for the burst we should expect to see very deep modulation due to rotation. The lack of a significant modulation in the burst profile indicates that we are either looking down at the magnetic pole or that the neutron star's rotation period is much greater than 10 s.

In the type I burster model, the burster must have a certain quiescent X-ray luminosity. The quiescent emission is generated from accretion of matter into the deep potential well of the neutron star. This gas subsequently undergoes nuclear fusion. Therefore, one expects the ratio of the quiescent lumi-

nosity to the mean burst luminosity to be the ratio of the potential energy of 1 gram of matter to the nuclear energy liberated from the same gram or about 25 (H-burning) or 100 (He-burning). Thus, the mean time between bursts, T, is expected to satisfy the following relation: $T \gtrsim \alpha E_B/L_Q$. Here E_B is the integrated energy of the burst and L_Q is the luminosity due to accretion, i.e., the luminosity of the source in quiescence.

From observation of the M28 region with the *ROSAT* High Resolution Imager (HRI) only two X-ray sources are found in the entire HRI field of view, the 3 ms radio pulsar RX J18245−2452P and RX J18245−2452E (Danner et al. 1997). These are separated by 10″ in the HRI images. However, at the resolution of the *ASCA* mirrors these two sources blend together and thus our *ASCA* source AX J18245−2451 is the sum of the two *ROSAT* sources. Danner et al. (1997) speculate that RX J18245−2452E is either a collection of low-luminosity point sources or a synchrotron nebula. An upper limit to the quiescent flux of the burster is thus a fraction of the luminosity of RX J18245−2452E—say, $L_Q \lesssim 10^{33}$ ergs s^{-1}. Given that the energy of our burst is $E_B \sim 3.1 \times 10^{37}$ ergs, we find $T \sim 0.1(\alpha/100)$ yr. This estimate of T is consistent with our lack of detections of any other burst from M28 in archival X-ray data from the *ROSAT* or *Einstein* missions.

5. SUMMARY

We have discovered a type I burst that is unique in two ways: (1) it is sub-Eddington by a factor of 100, and more importantly, (2) the quiescent luminosity of the source is 3 orders of magnitude smaller than that of all previously known bursters. We propose that these two observations can be explained by a model of a highly magnetized neutron star accreting at a low rate. The low accretion rate results in an Alfvén radius that is large and thus an equilibrium spin period that is concomitantly long (Bildsten & Brown 1997). This provides a natural explanation for the observed lack of any modulation in the burst profile despite the fact that the burst supposedly arises from a very small region.

Radio pulsars in globular clusters have a range of magnetic field strengths; see review by Kulkarni & Anderson (1996). These authors have argued that this observation can be explained by assuming that all cluster neutron stars are born with a distribution of magnetic field strengths similar to those in the disk (i.e., a typical dipole field strength of 10^{12} G). Depending on the accretion history a range of field strengths are then obtained. However, do note that Lyne, Manchester, & D'Amico (1996) disagree with this conclusion. Leaving aside this dissenting view, we note that in the picture of Kulkarni & Anderson highly magnetized neutron stars accreting matter at a low rate are expected to be quite common. Thus, a reasonable explanation can be found in this framework for the type of LMXB we hypothesized as the burst source discussed herein.

A natural consequence of this suggestion is that similar flashes should also be seen toward other clusters. Why have not such anomalous bursts been noticed before? We argue that previous nonimaging missions missed these bursts because of their limited dynamic range in sensitivity. Imaging telescopes have the sensitivity to detect such bursts. Unfortunately, the frequency of such flashes is low—a dozen per year per rich cluster. Discovery of another such burst from M28 would require 2 months of dedicated observations by *ASCA*! Thus, it will not be easy to verify this prediction. We eagerly look forward to the deployment of large field of view imaging monitors such as that proposed by Priedhorsky, Peele, & Nugent (1996).

Finally, we note that this class of bursts offers new insights into the physics of thermonuclear instabilities. For example, the fact that the quiescent luminosity is low enabled us to clearly recognize the afterglow. This phenomenon in itself is of interest to models of type I bursts. The afterglow could arise from extended burning (Fushiki et al. 1992) or slow propagation of the burning front (Bildsten 1995) or simply the emission from a transiently heated surface. The first two reasons have been advocated for conventional type I bursts but the latter is a new twist. It is important to note that the surface of the neutron stars in these systems is expected to be cooler than those of the brighter bursters, both because of a very small burst rate as well as a small quiescent luminosity. As remarked earlier, the value of the surface temperature (core temperature) is an important parameter in the theory of type I bursts. This opens the possibility that such bursts offer tests of the model over a range of previously unexplored parameter space.

E. V. G.'s research is supported by NASA. S. R. K.'s research is supported by NASA and NSF. S. R. K. thanks L. Bildsten and W. Lewin for education on the topic of bursters. We thank G. Hasinger, D. Helfand, E. S. Phinney, J. Swank, and F. Verbunt for helpful discussions, and K. Ebisawa for useful discussion concerning the GIS scaler data. This research has made use of data obtained through the HEASARC Online Service, provided by the NASA/GSFC.

REFERENCES

Bildsten, L. 1995, ApJ, 438, 852
Bildsten, L., & Brown, E. F. 1997, ApJ, 477, 897
Danner, R. M., Kulkarni, S. R., Saito, Y., & Kawai, N. 1997, Nature, 388, 751
Dotani, T., et al. 1990, Nature, 347, 534
Fujimoto, M. Y., Hanawa, T., & Miyaji, S. 1981, ApJ, 247, 267
Fushiki, I., Taam, R. E., Woosley, S. E., & Lamb, D. Q. 1992, ApJ, 390, 634
Garcia, M. R., & Grindlay, J. E. 1987, ApJ, 313, L59
Gotthelf, E. V. 1996, in *ASCA* News 4, HEASARC (Greenbelt: NASA/GSFC)
Gotthelf, E. V., Hamilton, T. T., & Helfand, D. J. 1996, ApJ 466, 779
Greiner, J., Duerbeck, H. W., & Gershberg, R. E., eds. 1994, Flares and Flashes (Berlin: Springer)
Joss, P. C., & Li, F. K. 1980, ApJ, 238, 287
Kulkarni, S. R., & Anderson, S. B. 1996, in IAU Symp. 174, Dynamical Evolution of Star Clusters, ed. P. Hut & J. Makino (Dordrecht: Klewer), 181
Lewin, W. G., van Paradijs, J., & Taam, R. E. 1993, Space Sci. Rev., 62, 223
Lyne, A. G., Brinklow, A., Middleditch, J. M., Kulkarni, S. R., Backer, D. C., & Clifton, T. R. 1987, Nature, 28, 399
Lyne, A. G., Manchester, R. N., & D'Amico, N. 1996, ApJ, 460, L41
Maraschi, L., & Cavaliere, A. 1977, in Highlights in Astronomy, Vol. 4, ed. E. A. Müller (Dordrecht: Reidel), 127
Priedhorsky, W. C., Peele, A. G., & Nugent, K. A. 1996, MNRAS, 279, 733
Rees, R. F., & Cudworth, K. M. 1991, AJ, 102, 152
Saito, Y., Kawai, N., Kamae, T., Shibata, S., Dotani, T., & Kulkarni, S. R. 1997, ApJ, 477, L37
Taam, R. E., & Picklum, R. E. 1978, ApJ, 224, 210
Tanaka, Y., Inoue, H., & Holt, S. S. 1994, PASJ, 46, L37
Woosley, S. E., & Taam, R. E. 1976, Nature, 263, 101

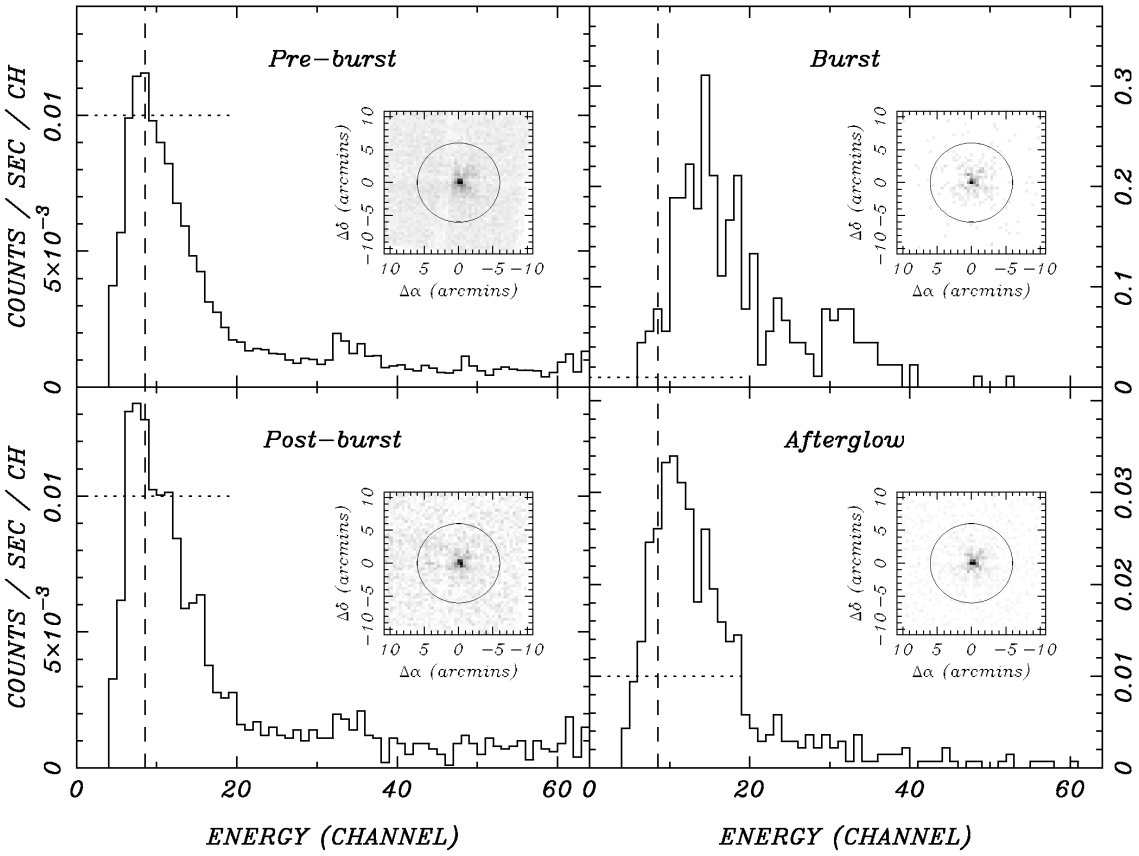

FIG. 2.—Combined SIS (SIS-0 + SIS-1) images and spectra of AX J18245−2451 obtained during the time intervals defined in Table 1: preburst (*top left*), flash (*top right*), afterglow (*bottom right*), and postburst (*bottom left*). The images are centered on the (same) measured centroid of AX J18245−2451 and display the entire 22′ × 22′ field of view of the SIS. The burst and afterglow images are consistent with a celestial point source (of equivalent counts) focused on the detectors. The 12′ diameter circle denotes the extraction region for the spectra plotted here, which are gain corrected and shown rebinned in units of ∼125 eV per bin. The dashed vertical line indicates the energy channel equivalent of 1 keV. The dashed horizontal line denotes a fiducial count rate of 0.01 counts s^{-1} per bin; the burst rate is almost 2 orders of magnitude higher then the quiescent rate. These results are perfectly reproduced by the GIS data (not shown).

GOTTHELF & KULKARNI (see 490, L162)

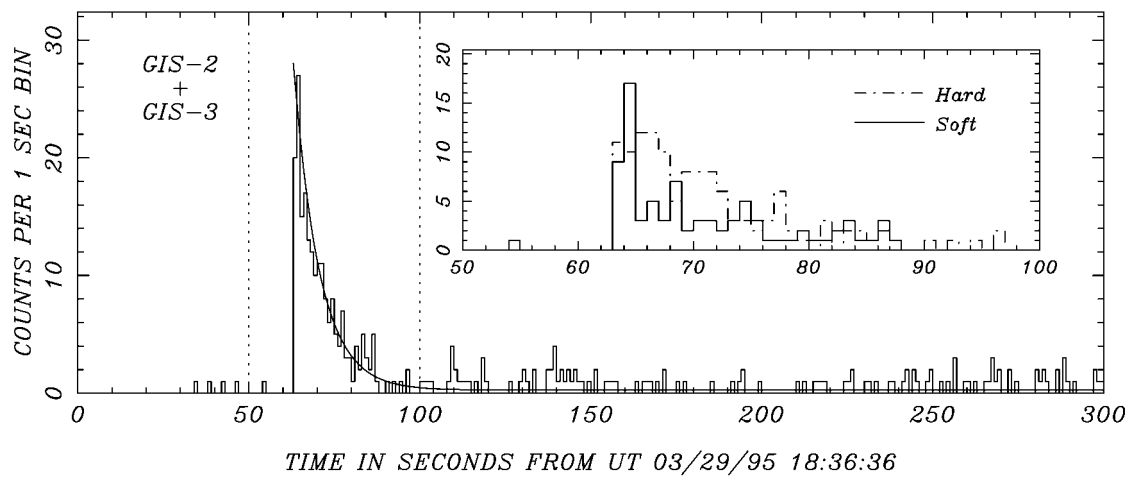

FIG. 3.—Combined GIS-2 and GIS-3 light curve binned in 1 s steps and centered on the prominent burst interval (*histogram*). The burst rise time is unresolved and is limited by counting statistics to more than 70 ms. The decay signal is well represented by an exponential model (*solid line*) with an *e*-folding time of τ = 7.5 s. (*Insert*) Spectrally resolved light curves. The dashed curves includes only photons with channel equivalent energy above 2 keV, whereas the solid histogram is for the remaining, soft photons. There is some indication of spectral evolution (see text).

GOTTHELF & KULKARNI (see 490, L162)